

An automated procedure for determining asymptotic elastic stress fields at singular points

Donghee Lee and J R Barber*

Department of Mechanical Engineering, University of Michigan, Ann Arbor, Michigan, USA

The manuscript was received on 8 September 2005 and was accepted after revision for publication on 17 January 2006.

DOI: 10.1243/03093247JSA164

Abstract: The paper describes an analytical tool in MATLAB for determining the nature of the stress and displacement fields near a fairly general singular point in linear elasticity. The user is prompted to input the local geometry of the system, the material properties, and the boundary conditions (and interface conditions in the case of composite bodies or problems involving contact between two or more bodies). The tool then computes the dominant eigenvalue and provides as output the equations defining the singular stress and displacement fields and contour plots of these fields. No knowledge of the asymptotic analysis procedure is required of the user.

The tool is tested against previously published results where available and proves to be robust and accurate. It is potentially useful for the development of special finite elements for singular points or for characterizing failure at such points. It can be downloaded from the website <http://www-personal.umich.edu/~jbarber/asymptotics/intro.html>

Keywords: wedge, asymptotic, singularity, automation

1 INTRODUCTION

Singular stress fields are generally developed in elastic bodies at re-entrant corners (sharp notches and cracks) and at the end points of discontinuous interfaces between dissimilar bodies. Some typical examples are shown in Fig. 1. Williams [1] pioneered the technique of asymptotic analysis in which the local stress field is expanded as a series, each term of which has power-law dependence on r , where (r, θ) is a system of polar coordinates based on the singular point. As the singular point is approached, the field will be increasingly dominated by the leading term in this series, i.e. the term for which the power-law exponent is smallest (or has the smallest real part). Thus, if failure is determined by behaviour in a small region near the singular point, it will be characterized simply by the coefficient of this most singular term [2]. In the case of a crack, this coefficient is the familiar stress intensity factor, which forms the basis of linear elastic fracture mechanics (LEFM). Similar arguments have been used to predict local failure

in other situations involving theoretically singular elastic fields, such as a notch [3, 4] or fretting fatigue at a sharp corner [5, 6].

Knowledge of the nature of the singular field is also important in numerical (typically finite element) solutions of elasticity problems involving singular points [7]. Conventionally, a highly refined mesh will be used in such regions in the hope of capturing the nature of the local field, but this approach is extremely computer-intensive and even then may fail to converge with increasing mesh refinement, thus compromising the entire numerical solution. The most efficient way to solve such problems is to define a special element to model the region immediately surrounding the singular point [8]. The shape function used in this element can then be chosen to conform with that of the dominant singular term in the appropriate asymptotic expansion. Special elements for crack tips in homogeneous materials are now included in all the major commercial finite element codes and several authors have developed and used special elements in other situations involving singular points [9–12].

Results for the asymptotic fields in a variety of special cases have been published. Bogy [13] investigated the case of bonded dissimilar wedges and in a

* Corresponding author: Department of Mechanical Engineering, University of Michigan, 2350 Hayward Street, Ann Arbor, Michigan 48109-2125, USA. email: jbarber@engin.umich.edu

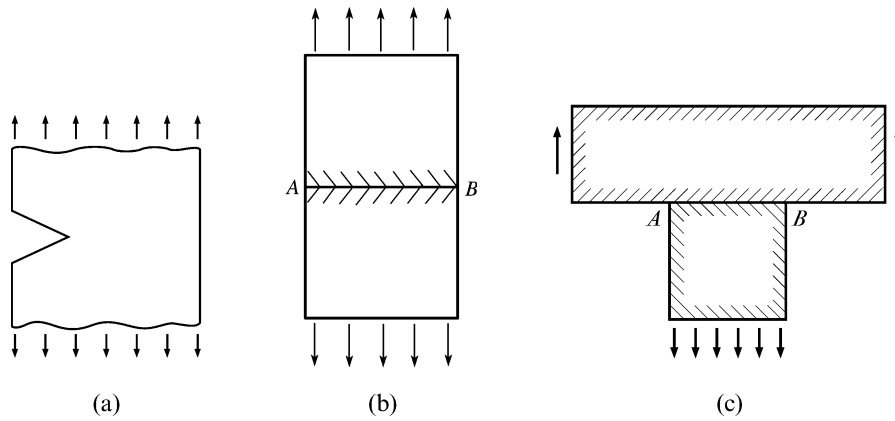


Fig. 1 Elastic structures involving singular points

discussion to this paper Dundurs [14] demonstrated that a more efficient statement of the solution could be made in terms of the now well-known Dundurs' parameters [see equations (18) and (19) below]. Further results for this system were then given by Bogy [15] and Bogy and Wang [16]. The asymptotic field at the corner of a sharp body indenting an elastic half-plane was investigated by Dundurs and Lee [17] for the frictionless case and the corresponding frictional problem was considered by Gdoutos and Theocaris [18] and Comninou [19]. It should be noted that apart from the results of Williams, which can be presented in a convenient graphical form, it is far from easy to use these published results to determine the power-law exponent, since the authors generally use an inverse method to obtain their results.

The general technique of asymptotic analysis at a singular point is now a well-established branch of elasticity [20], but the algebraic calculations can be tedious and time consuming and are usually a distraction from the main purpose of the investigation for which they are required. For this reason, many investigators simply use conventional elements with mesh refinement at singular points, often even without the backup of an appropriate convergence test. In the present paper, an automated procedure is introduced for solving the asymptotic eigenvalue problem for a fairly general class of singular point, using the software code MATLABTM. Potential users merely need to specify the geometrical description of the singular point and the appropriate material properties and boundary conditions. The program then solves the eigenvalue problem, determining the strength of the dominant singular term and the form of the stress and displacement fields in the dominant region.

2 SOLUTION METHOD

First a set of polar coordinates centred on the singular point is defined before focusing on a region extremely close to the origin, which is equivalent to looking at the singular point through a very strong microscope. In this view, all the other geometric features of the component appear to be far distant from the origin and any curved boundaries in the field of vision will appear straight because their radii of curvature will have been indefinitely magnified. The local elasticity problem therefore reduces to that of one or more semi-infinite wedges with appropriate boundary conditions at the terminal edges $\theta = \alpha_1$ and $\theta = \alpha_2$ and at the interface(s) $\theta = \beta_1$ and $\theta = \beta_2, \dots$ (if any) between adjacent wedges. This will be referred to as the 'asymptotic problem'.

2.1 Boundary and interface conditions

The only finite boundaries in the asymptotic problem comprise the two edges $\theta = \alpha_1$ and $\theta = \alpha_2$. At an edge $\theta = \alpha$, the boundary conditions might take any one of the following forms

B(i): traction-free

$$\sigma_{\theta r}(r, \alpha) = 0; \quad \sigma_{\theta\theta}(r, \alpha) = 0 \quad (1)$$

B(ii): bonded to a rigid body

$$u_r(r, \alpha) = 0; \quad u_\theta(r, \alpha) = 0 \quad (2)$$

B(iii): frictionless contact with a rigid body

$$\sigma_{\theta r}(r, \alpha) = 0; \quad u_\theta(r, \alpha) = 0 \quad (3)$$

B(iv): frictional contact with a rigid body

$$\sigma_{\theta r}(r, \alpha) \pm f\sigma_{\theta\theta} = 0; \quad u_\theta(r, \alpha) = 0 \quad (4)$$

where the sign in the first equation depends on the assumed direction of slip.

At an interface $\theta = \beta$ between the j th and $(j + 1)$ th wedges, equilibrium conditions demand that

$$\begin{aligned} \sigma_{\theta r}^j(r, \beta) - \sigma_{\theta r}^{(j+1)}(r, \beta) &= 0 \\ \sigma_{\theta\theta}^j(r, \beta) - \sigma_{\theta\theta}^{(j+1)}(r, \beta) &= 0 \end{aligned} \tag{5}$$

In addition, depending on the status of the interface, the additional conditions are as follows

I(i): bonded interface

$$u_r^j(r, \alpha) - u_r^{(j+1)}(r, \alpha) = 0; \quad u_\theta^j(r, \alpha) - u_\theta^{(j+1)}(r, \alpha) = 0 \tag{6}$$

I(ii): frictionless contact

$$\sigma_{\theta r}^j(r, \beta) = 0; \quad u_\theta^j(r, \alpha) - u_\theta^{(j+1)}(r, \alpha) = 0 \tag{7}$$

I(iii): frictional contact

$$\sigma_{\theta r}^j(r, \beta) \pm f\sigma_{\theta\theta}^j(r, \beta) = 0; \quad u_\theta^j(r, \alpha) - u_\theta^{(j+1)}(r, \alpha) = 0 \tag{8}$$

where the sign in the first equation depends on the assumed direction of slip. At the most general singular point, there will be n wedges, $n - 1$ interfaces, and two edges, in which case the appropriate choice from equations (1) to (8) defines $4n$ homogeneous conditions that must be satisfied by the stress fields in the wedges.

By way of illustration, Fig. 2 shows the asymptotic problem corresponding to the singular point A in Fig. 1. There are two wedges of dissimilar materials occupying the regions $-\pi/2 < \theta < 0$ and $0 < \theta < \pi$ respectively. There are two traction-free boundaries [equation (1)] corresponding to $\alpha_1 = -\pi/2$ and $\alpha_2 = \pi$ and one bonded interface [equation (6)] $\beta = 0$.

2.2 Asymptotic expansion

The asymptotic problem is self-similar (there is no inherent length scale) and the boundary and interface conditions are all homogeneous. Particular

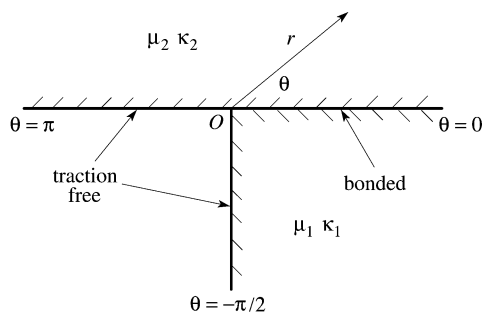


Fig. 2 Asymptotic problem corresponding to point A in Fig. 1(c)

solutions are therefore sought for the governing equations of elasticity in which the displacement fields have the separated-variable form

$$u = r^\lambda f(\theta) \tag{9}$$

The most general solution of this kind in the wedge j is conveniently expressed in terms of the Airy stress function [20]

$$\begin{aligned} \phi = r^{\lambda+1} [&A_j \cos(\lambda + 1)\theta + B_j \cos(\lambda - 1)\theta \\ &+ C_j \sin(\lambda + 1)\theta + D_j \sin(\lambda - 1)\theta] \end{aligned} \tag{10}$$

corresponding to the stress and displacement components

$$\begin{aligned} \sigma_{rr} = r^{\lambda-1} [&-A_j \lambda(\lambda + 1) \cos(\lambda + 1)\theta \\ &-B_j \lambda(\lambda - 3) \cos(\lambda - 1)\theta \\ &-C_j \lambda(\lambda + 1) \sin(\lambda + 1)\theta \\ &-D_j \lambda(\lambda - 3) \sin(\lambda - 1)\theta] \end{aligned} \tag{11}$$

$$\begin{aligned} \sigma_{r\theta} = r^{\lambda-1} [&A_j \lambda(\lambda + 1) \sin(\lambda + 1)\theta \\ &+ B_j \lambda(\lambda - 1) \sin(\lambda - 1)\theta \\ &-C_j \lambda(\lambda + 1) \cos(\lambda + 1)\theta \\ &-D_j \lambda(\lambda - 1) \cos(\lambda - 1)\theta] \end{aligned} \tag{12}$$

$$\begin{aligned} \sigma_{\theta\theta} = r^{\lambda-1} [&A_j \lambda(\lambda + 1) \cos(\lambda + 1)\theta \\ &+ B_j \lambda(\lambda + 1) \cos(\lambda - 1)\theta \\ &+ C_j \lambda(\lambda + 1) \sin(\lambda + 1)\theta \\ &+ D_j \lambda(\lambda + 1) \sin(\lambda - 1)\theta] \end{aligned} \tag{13}$$

$$\begin{aligned} 2\mu_j u_r = r^\lambda [&-A_j (\lambda + 1) \cos(\lambda + 1)\theta \\ &+ B_j (\kappa_j - \lambda) \cos(\lambda - 1)\theta \\ &-C_j (\lambda + 1) \sin(\lambda + 1)\theta \\ &+ D_j (\kappa_j - \lambda) \sin(\lambda - 1)\theta] \end{aligned} \tag{14}$$

$$\begin{aligned} 2\mu_j u_\theta = r^\lambda [&A_j (\lambda + 1) \sin(\lambda + 1)\theta \\ &+ B_j (\kappa_j + \lambda) \sin(\lambda - 1)\theta \\ &-C_j (\lambda + 1) \cos(\lambda + 1)\theta \\ &-D_j (\kappa_j + \lambda) \cos(\lambda - 1)\theta] \end{aligned} \tag{15}$$

where A_j, B_j, C_j, D_j are arbitrary constants, μ_j is the shear modulus, and κ_j is Kolosov's constant equal to $3 - 4\nu_j$ in plane strain and $(3 - \nu_j)/(1 + \nu_j)$ in plane stress, with ν_j being Poisson's ratio.

Substitution of these results into the appropriate boundary and interface conditions (1) to (8) will yield $4n$ homogeneous linear algebraic equations for the $4n$ unknowns A_j, B_j, C_j, D_j . For most values of λ , these equations will have only the trivial solution $A_j = B_j = C_j = D_j = 0$, but non-trivial solutions are

obtained for a denumerably infinite set of eigenvalues λ_i at which the algebraic equations are not linearly independent. These eigenvalues are the solutions of the characteristic equation obtained by setting the determinant of the coefficients of the algebraic equations to zero. Depending on the conditions at the singular point, the eigenvalues λ_i may be real or complex.

2.3 Eigenfunctions

For each eigenvalue λ_i there is an associated eigenfunction that can be found by eliminating the redundant equation from the set and solving for $4n - 1$ of the constants in terms of the remaining constant. Substitution into equations (10) to (15) then defines a non-trivial particular solution to the asymptotic problem of the form

$$\mathbf{u} = K_i r^{\lambda_i} \mathbf{f}_i(\theta) \quad (16)$$

where K_i is the one remaining undetermined multiplying constant. A more general solution to the asymptotic problem can then be written in the form of the eigenfunction expansion

$$\mathbf{u} = \sum_{i=1}^{\infty} K_i r^{\lambda_i} \mathbf{f}_i(\theta) \quad (17)$$

Gregory [21] has shown that this expansion is complete for the problem of the single wedge loaded only on the circular boundary $r = a$. It must also therefore be complete for the local field at a traction-free notch in an arbitrarily shaped body, since the imaginary boundary $r = a$ in that body must transmit a unique set of tractions. To the best knowledge of the present authors, rigorous completeness proofs are not available for more general singular points, but it seems likely that this representation has general validity.

If the strain energy in the body is to be bounded, all the eigenvalues must satisfy the condition $\Re(\lambda_i) > 0$ [20] and if they are ranked in order of increasing real part, the stress field in the immediate vicinity of the singular point will be dominated by the first term $K_0 r^{\lambda_0} \mathbf{f}_0(\theta)$. This term will define a singular field if and only if $0 < \Re(\lambda_0) < 1$.

3 ANALYTICAL TOOL

This procedure has been automated using the software code MATLABTM v.7.1 with the MATLAB GUI Development Environment (GUIDE) v.2.5 and the MATLAB Symbolic Toolbox v.3.1. The analytical tool provides a graphic interface in which users can define their problem, determine the order of the

corresponding singularity, and generate the distribution of stress and displacement. Final results are provided in both text and graphic format.

Figure 3 shows a schematic of the steps involved in the solution. Users specify the geometry of the singular point through the angles α_1, α_2 defining the edges, and the angles β_1, β_2, \dots defining the interfaces between regions (wedges) of different materials, if any. They also specify the material properties μ_j, ν_j of the various regions and whether conditions are plane strain or plane stress. Finally, for each edge or interface, they select one of the qualitative states itemized in section 2.1.

Using this input, the analytical tool constructs the corresponding system of algebraic equations and hence determines the characteristic equation by evaluating the determinant of coefficients. It then attempts to solve this equation to evaluate the first few eigenvalues, using MapleTM (which is included as a solver within MATLAB). If the characteristic equation system is too complicated for Maple to solve, the user is prompted to use Newton's method to obtain an iterative solution. Since the characteristic equation has many solutions, the result of this iterative procedure is sensitive to the choice of initial guess, so a visual root finder is provided in order that the user can make a selection of an appropriate initial guess. This procedure is explained in section 3.3 below.

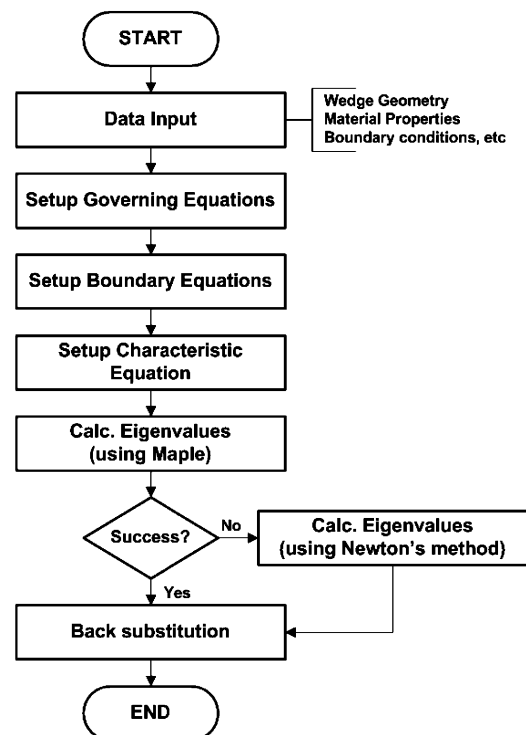


Fig. 3 Flowchart for the automated eigenvalue solver

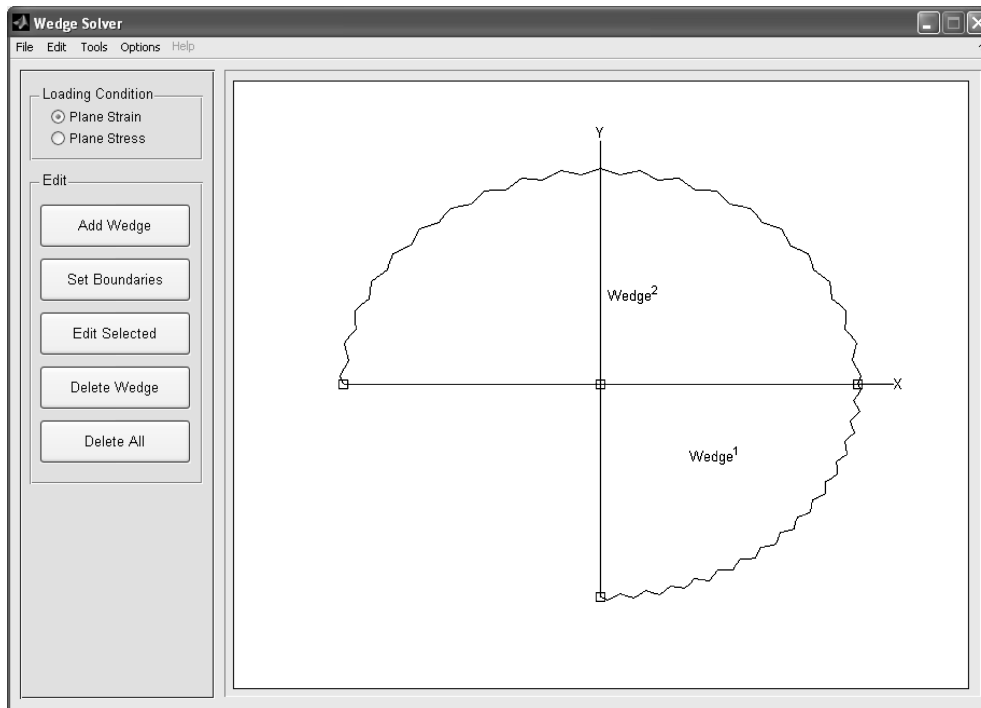


Fig. 4 Geometry of the asymptotic problem of Fig. 2

Once the lowest eigenvalue has been determined, the corresponding eigenfunction is obtained by the back-substitution procedure of section 2.3. Features of the corresponding stress or displacement field can then be displayed as contour plots.

3.1 Data input

Figure 4 shows the graphic interface representing the appropriate geometry for the asymptotic problem of Fig. 2. On starting the program, the user is presented with a blank screen of this form, in which they first select plane stress or plane strain as appropriate. Clicking on 'Add Wedge' opens an input window for the first wedge as shown in Fig. 5. For the present example, $-\pi/2$ and 0 would be selected to define the wedge angles and then input the appropriate material properties for material 1. If the box 'Use Loading Condition' is clicked, Kolosov's constant κ will be calculated from ν based on the previously specified loading condition. Alternatively, if this box is not checked, κ can be input as an independent variable.

Clicking on 'Ok' returns the user to the geometry window, in which the first wedge will now be correctly identified. To add the second wedge, again click on 'Add Wedge' and enter the angles 0 and π and the properties of material 2, which will then return to the geometry window in the form shown in Fig. 4.

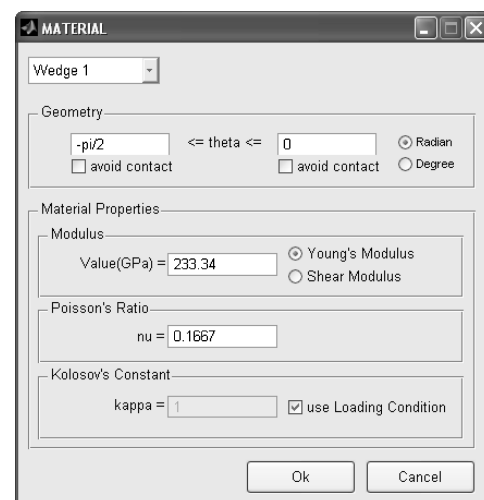


Fig. 5 Input window for the first wedge

There is no limitation on the number of wedges that can be entered into the problem statement using this procedure, but the algebraic complexity of multiwedge problems may place practical limits, depending on the available hardware resources such as processor and memory capacity.

3.2 Boundary and interface conditions

Once the geometry of the problem is completely specified, the next step is to identify the conditions at the boundaries and interfaces by selecting between

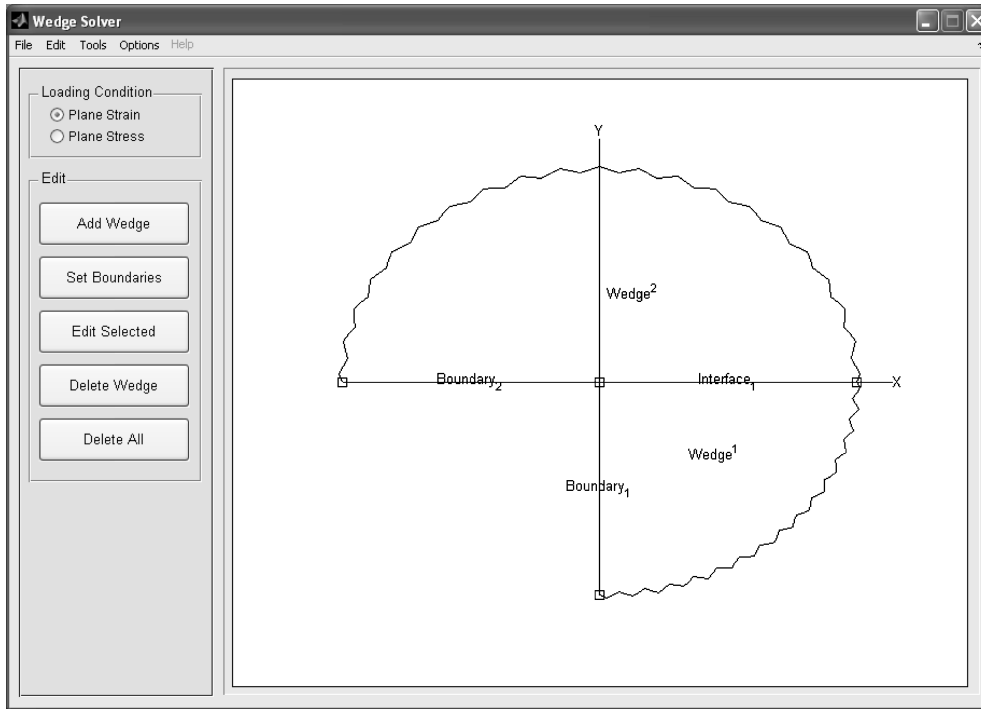


Fig. 6 Geometry of the problem with boundaries and interfaces identified

the choices in section 2.1. The first step is to click on the button ‘Set Boundaries’ in Fig. 4, leading to the screen of Fig. 6, in which all the boundaries and interfaces are identified and sequentially numbered. The default option is to identify radial lines shared by two wedges as interfaces. The user can override this assumption by checking the box ‘Avoid Contact’ for the appropriate edge in the wedge input window of Fig. 5. The user next highlights one of the boundaries using the mouse and clicks on ‘Edit Selected’. This opens a data input window, which in the case of a boundary offers the choice of the boundary conditions B(i) to B(iv) in section 2.1, as shown in Fig. 7. If ‘Frictional Contact with a Rigid Body’ is selected, the coefficient of friction f must

also be input. Notice that f may take either sign depending on the direction of slip anticipated at the singular point. In general, different singular fields are obtained for different directions of slip. If an interface is highlighted at this stage, the corresponding data input window offers the choices I(i) to I(iii) in section 2.1.

3.3 Solving process

To start the solution of the eigenvalue problem, the user clicks on ‘Tools → Run’ in the toolbar of Fig. 6. During the solution, a message window is shown on the screen to inform the user of the progress of the solution. Once the characteristic equation has been constructed, the tool will attempt to solve it using Maple. However, sometimes this is unsuccessful and an iterative numerical solution is necessary, using Newton’s method. The success of this method depends on the choice of initial guess. To increase reliability, the user is prompted to select an appropriate initial value by the root-finding screen shown in Fig. 8.

Figure 8 shows the loci of the equations $\Re\{\mathcal{C}(\lambda)\} = 0$ (solid lines) and $\Im\{\mathcal{C}(\lambda)\} = 0$ (dashed lines), where $\mathcal{C}(\lambda) = 0$ is the characteristic equation. The loci are plotted in the complex plane for λ , so that real eigenvalues (if any) appear on the real axis. Both these equations must be satisfied, so permissible eigenvalues correspond to the intersection of a

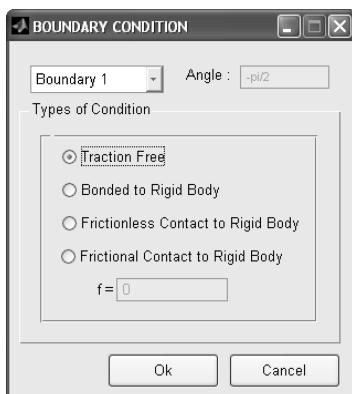


Fig. 7 Data input window for boundary 1 from Fig. 6

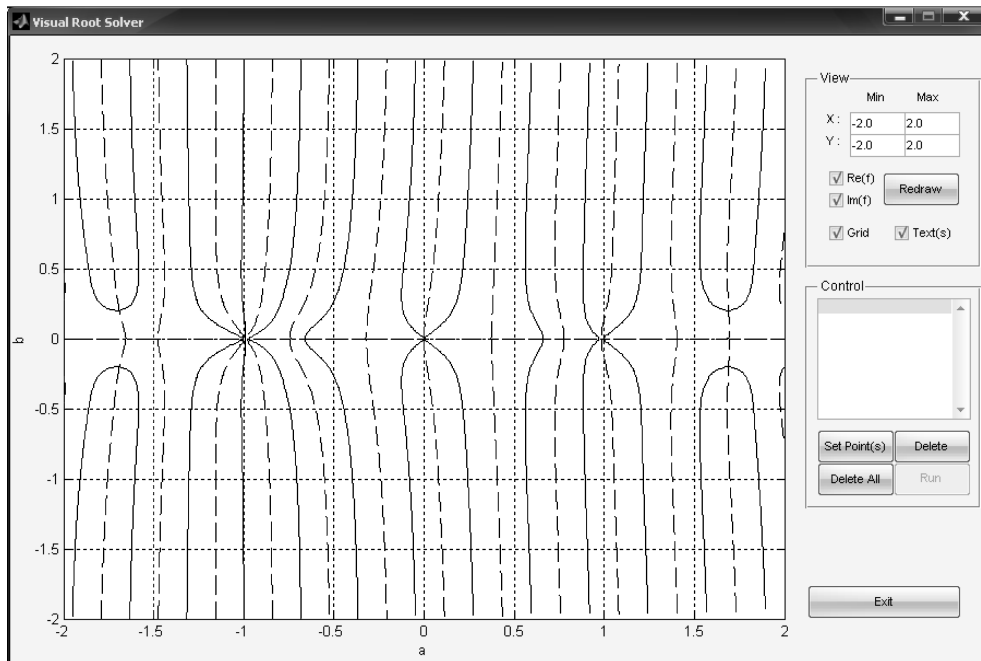


Fig. 8 Visual root finder

pair of solid and dashed lines. To select a point near to the required intersection, the user clicks on the 'Set Point(s)' button in Fig. 8 and then moves the mouse to click on the appropriate intersection. The coordinates of the point selected are displayed in the box at the bottom right of the screen. More than one point may be selected if desired, in which case all the resulting eigenvalues will be returned. Once the initial value has been identified, the user clicks on the right mouse button and then on 'Exit', which closes this screen and returns to the solving process.

3.4 Presentation of results

Once the solution process is complete, the tool returns a 'Results' screen from which the user can select to display the governing equations, the equations derived from the boundary and interface conditions, the characteristic equation, and the eigenvalue(s). Selection of the options in the 'Results of Back Substitution' frame provides a text description of the equations defining the eigenfunction field for stress or displacement components associated with the eigenvalue with the smallest real part and a contour plot of the same fields.

4 VALIDATION

To demonstrate the usefulness of the tool and to evaluate its robustness, it was tested by comparison

with the results for (a) the single wedge solution of Williams [1], (b) the bonded dissimilar wedge problem of Bogy [15], and (c) the frictional contact problem of Gdoutos and Theocaris [18]. In each case, the lowest eigenvalues obtained agreed exactly with those given by the original authors (including the imaginary part of the eigenvalue in cases where this is complex). For example, the tool was used to determine the eigenvalues for the system of Fig. 2. Following Bogy [15], the results are presented in Fig. 9 as a contour plot of the real and imaginary parts of the dominant eigenvalue as functions of Dundurs' parameters.

5 CONCLUSIONS

An analytical tool has been developed within MATLAB for solving the asymptotic problem for a fairly general class of singular points in linear elasticity. The tool does not require any specialist knowledge of asymptotic analysis and it provides as output the power of the dominant singular term (the eigenfunction) and the form of the resulting stress and displacement fields. The tool has been tested against previously published asymptotic solutions and in all cases it gives reliable and accurate results. It should also be remarked that most of these previous solutions resort to an inverse method for determining the eigenvalues. In other words, they specify the eigenvalue and solve for the corresponding

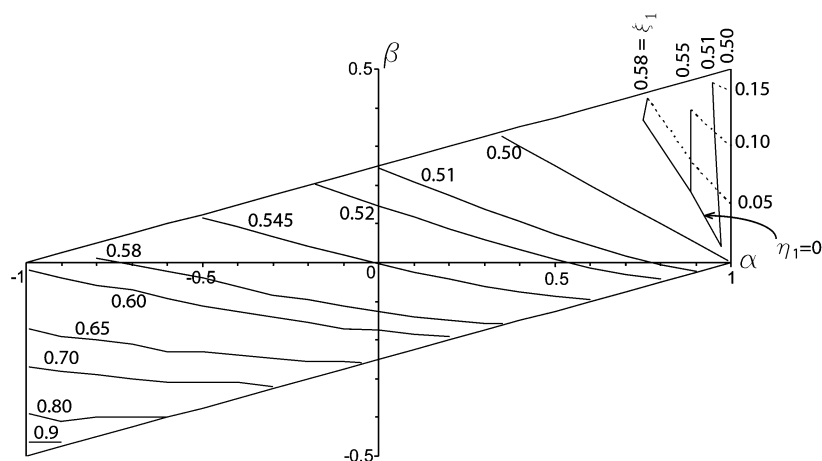


Fig. 9 Contour plot of eigenvalues for the problem of Fig. 2

material properties. The present solution is direct, which is more likely to be useful in particular applications. The results are potentially useful for the development of special finite elements or other efficient numerical strategies for problems involving singular points. The source code can be downloaded from the website <http://www-personal.umich.edu/~jbarber/asymptotics/intro.html>

REFERENCES

- 1 Williams, M. L. Stress singularities from various boundary conditions in angular corners of plates in extension. *Trans. ASME, J. Appl. Mechanics*, 1952, **19**, 526–528.
- 2 Dunn, M. L. Fracture initiation at geometric and material discontinuities: criteria based on critical stress intensities of linear elasticity. *Chin. J. Mechanics A*, 2003, **19**, 15–29.
- 3 Leguillon, D. Strength or toughness? A criterion for crack onset at a notch. *Eur. J. Mechanics A/Solids*, 2002, **21**, 61–72.
- 4 Lazzarin, P., Lassen, T., and Livieri, P. A notch stress intensity approach applied to fatigue life predictions of welded joints with different local toe geometry. *Fatigue Fract. Engng Mater. Structs*, 2003, **26**, 49–58.
- 5 Giannakopoulos, A. E., Lindley, T. C., and Suresh, S. Aspects of equivalence between contact mechanics and fracture mechanics: theoretical connections and a life-prediction methodology for fretting-fatigue. *Acta Mater.*, 1998, **46**, 2955–2968.
- 6 Churchman, C., Mugadu, A., and Hills, D. A. Asymptotic results for slipping complete frictional contacts. *Eur. J. Mechanics A/Solids*, 2003, **22**, 793–800.
- 7 Sinclair, G. B., Cormier, N. G., Griffi, J. H., and Meda, G. Contact stresses in dovetail attachments: finite element modeling. *Trans. ASME, J. Engng Gas Turbine Power*, 2002, **124**, 182–189.
- 8 Seweryn, A. Modeling of singular stress fields using finite element method. *Int. J. Solids Structs*, 2002, **39**, 4787–4804.
- 9 Lin, V. and Tong, P. Singular finite elements for the fracture analysis of V-notched plate. *Int. J. Numer. Meth. Engng*, 1980, **15**, 1343–1354.
- 10 Chen, M.-C. and Sze, K. Y. A novel finite element analysis of bimaterial wedge problems. *Engng Fract. Mechanics*, 2001, **68**, 1463–1476.
- 11 Tur, M., Fuenmayor, J., Mugadu, A., and Hills, D. A. On the analysis of singular stress fields. Part 1: finite element formulation and application to notches. *J. Strain Analysis*, 2002, **37**(5), 437–444.
- 12 Liu, C. H. and Huang, C. Oscillatory crack tip triangular elements for finite element analysis of interface cracks. *Int. J. Numer. Meth. Engng*, 2003, **58**, 1765–1783.
- 13 Bogy, D. B. Edge-bonded dissimilar orthogonal elastic wedges under normal and shear loading. *Trans. ASME, J. Appl. Mechanics*, 1968, **35**, 460–466.
- 14 Dundurs, J. Discussion on edge bonded dissimilar orthogonal elastic wedges under normal and shear loading. *Trans. ASME, J. Appl. Mechanics*, 1969, **36**, 650–652.
- 15 Bogy, D. B. Two edge-bonded elastic wedges of different materials and wedge angles under surface tractions. *Trans. ASME, J. Appl. Mechanics*, 1971, **38**, 377–386.
- 16 Bogy, D. B. and Wang, K. C. Stress singularities at interface corners in bonded dissimilar isotropic elastic materials. *Int. J. Solids Structs*, 1971, **7**, 993–1005.
- 17 Dundurs, J. and Lee, M. S. Stress concentration at a sharp edge in contact problems. *J. Elasticity*, 1972, **2**, 109–112.
- 18 Gdoutos, E. E. and Theocaris, P. S. Stress concentrations at the apex of a plane indenter acting on an elastic half plane. *Trans. ASME, J. Appl. Mechanics*, 1975, **42**, 688–692.
- 19 Comninou, M. Stress singularity at a sharp edge in contact problems with friction. *Z. Angew. Math. Phys.*, 1976, **27**, 493–499.

- 20 Barber, J. R.** *Elasticity*, 2nd edition, 2002, section 11.2 (Kluwer, Dordrecht, The Netherlands).
- 21 Gregory, R. D.** Green's functions, bi-linear forms and completeness of the eigenfunctions for the elastostatic strip and wedge. *J.Elasticity*, 1979, **9**, 283–309.

\mathbf{u}	displacement fields near the singular point
u_r, u_θ	displacement components near the singular point
α, β	Dundurs' constants in equations (18) and (19)
α_i, β_i	angular position of the boundary and interface
κ	Kolosov's constant
λ	eigenvalue
μ	shear modulus
$\sigma_{rr}, \sigma_{r\theta}, \sigma_{\theta\theta}$	stress components near the singular point
ϕ	Airy stress function

APPENDIX

Notation

f	friction coefficient
K_i	undetermined multiplying constant
r, θ	polar coordinates based on the singular point